

4 Background information

4.1 Titanium dioxide

Titanium dioxide is a non-toxic, wide band gap semiconductor, which is most commonly used as a white pigment in tooth paste, wall paint, white paper, etc. The material has many unique properties due to its extraordinary chemical stability. When excited with UV-irradiation, it can be employed as a photocatalyst to split water, as an anti-foggy coating on glass surfaces (mirror, window pane, etc) or as an anti-bacterial coating on various substrates. The potential of the holes in the valence band is sufficiently low to oxidate most organic compounds, which is a reason why it is widely employed on self-cleaning surfaces. In contrast to other semiconductors with similar band gaps (e.g. ZnO), it does not photo-degrade upon excitation.

The scientifically and technologically most relevant modifications of titanium dioxide are anatase, rutile and brookite, which have the following crystallographic properties:

- 1) anatase (space group $I4_1/amd$, symmetry D_{4h})
- 2) rutile (space group $P4_2/mnm$, symmetry D_{4h})
- 3) brookite (space group $Pbca$, symmetry D_{2h})

Other modifications, that have been synthesized, are [127]:

- 4) TiO_2 II (“columbite”, (α - PbO_2) space group $Pbcn$),
- 5) TiO_2 III (“baddeleyite”, space group $P2_1/c$)
- 6) TiO_2 (H) (“hollandite”, space group $I4/m$),
- 7) TiO_2 (R) (“ramsdellite”, space group $Pbnm$)
- 8) TiO_2 (B) (“bronze”, space group $C2/m$)

Except TiO_2 (B), none of the latter modifications occur in nature. They have been mostly synthesized by high pressure treatment of anatase or rutile.

Formally, titanium dioxide is made up of d^0 titanium ions (charge +IV) at the center of an octahedron of six O^{2-} -ions. The most important modifications anatase and rutile mainly differ by the distortion inside the octahedron. The unit cell of anatase and rutile are shown in Fig. 4.1 Anatase has a density of $3.8 - 4 \text{ gcm}^{-3}$, which is a little bit less than rutile with a density of $4.2 - 4.3 \text{ gcm}^{-3}$. The average distance between the Ti^{4+} -ions in anatase is smaller compared to rutile, which makes it thermodynamically less stable. Hartree-Fock calculations [128] have shown that the enthalpy of formation is about $1.2 - 2.8 \text{ kcal}$ higher for anatase. However, the phase transition from anatase to rutile needs a significant thermal activation and occurs between $700 - 1000 \text{ }^\circ\text{C}$ depending on the crystal size and the impurity content [129].

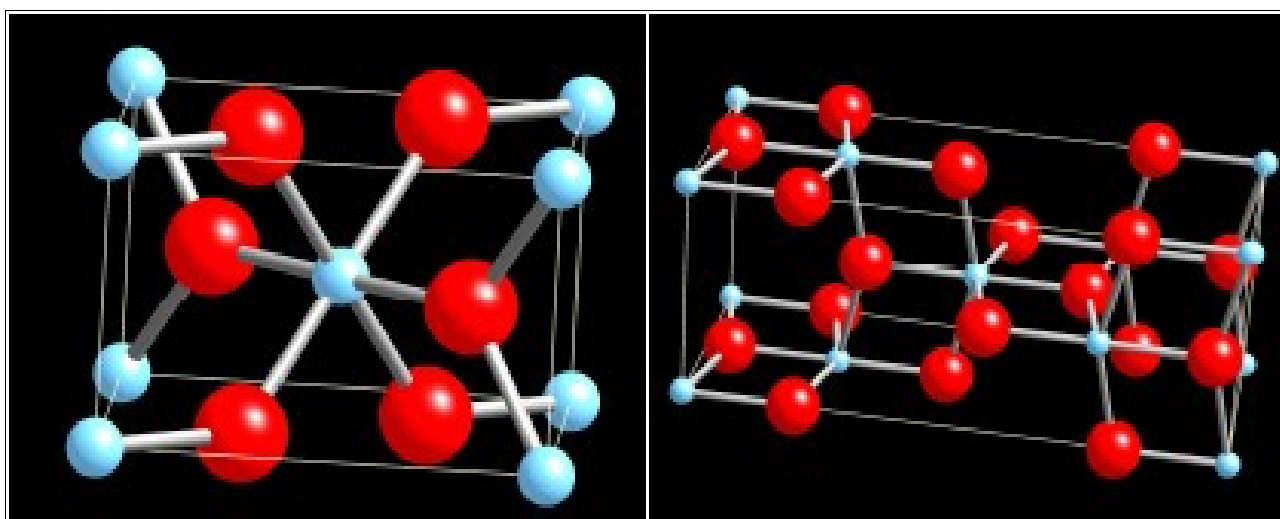


Fig. 4.1: unit cell of a) anatase and b) rutile

For dye-sensitized solar cells (DSSC) the use of nanoporous anatase has been proven to be superior to rutile. There is no generally accepted explanation for this finding. It is believed to be related to the structure and chemical composition of the TiO_2 -surface. For single-crystal anatase and rutile the injection efficiency was found to be the same [127]. The most common lattice planes in anatase is (101) followed by (100) and (001) [130]. For rutile the most common lattice plane is (100) [127]. By UV-VIS spectroscopy the indirect bandgap of anatase (101) was determined to be 3.2 eV compared to 3.0 eV for rutile (100) [127]. The difference is attributed to a negative shift of the conduction band in anatase by 0.2 eV , whereas the position of the valence band remains unaffected [127]. On an absolute scale, the position of the anatase conduction band is given with

-4.4 eV [131].

The bonding within titanium dioxide is partly covalent and partly ionic. Therefore stoichiometric crystals are insulating. However, most synthesis routes induce a significant amount of trap states, that are due to oxygen vacancies. These vacancies can also be formed reversibly under reduced pressure [132] and/or elevated temperature [133]. As a consequence the conductivity can vary by several orders of magnitude. For example, the conductivity of porous anatase electrodes increases from $5 \cdot 10^{-9} \Omega^{-1} \text{cm}^{-1}$ (room temperature, ambient atmosphere) to $1 \cdot 10^{-6} \Omega^{-1} \text{cm}^{-1}$ (partial oxygen pressure $p_{\text{O}_2} = 0.02$, $T = 400 \text{ }^\circ\text{C}$) [134]. The oxygen vacancies cause the formation of Ti^{3+} -state, which dope the crystal negatively.

The flat band potential of TiO_2 in aqueous solution is known to depend strongly on the pH. Since the surface of TiO_2 -crystals is typically OH-terminated, the interaction with water is strong. Effusion of water is observed up to $400 \text{ }^\circ\text{C}$ [134]. Assuming a Nernstian-type pH-dependence, a shift of 59 mV/pH would be expected [135]. However, the shift for real electrodes can be both smaller or bigger depending on the density of trap states and the surface morphology [136].

In general, the shift of the TiO_2 flat band potential by electron withdrawing/inducing coadsorbents is a commonly applied concept in the optimization of DSSC [137].

Single crystals of rutile are widely available. Several companies (Kelpin Kristallhandel, Germany, Commercial Crystal laboratory, USA, Goodfellow, UK) provide high purity crystals on a large scale. Thus most often the crystals are bought and cut in the laboratory to investigate the desired lattice plane.

The synthesis of anatase is more complicated, since it is metastable. The temperature during the reaction must not exceed a certain threshold to avoid the phase transition to rutile. Most commonly gas phase reactions with halides (HCl , HBr , CCl_4 and TeCl_4) as the transport agent are applied [127].

Crystals on the sub-microscopic scale are usually made by spraypyrolysis [138], electrodeposition [139] or hydrolysis of organic Ti^{IV} -precursors and successive autoclaving [140]. The commercially most common product is P25 from Degussa, which is a TiO_2 -powder with 25 nm particle diameter in average. It is synthesized by flame hydrolysis and consist of ca. 70 % anatase and 30 % rutile.

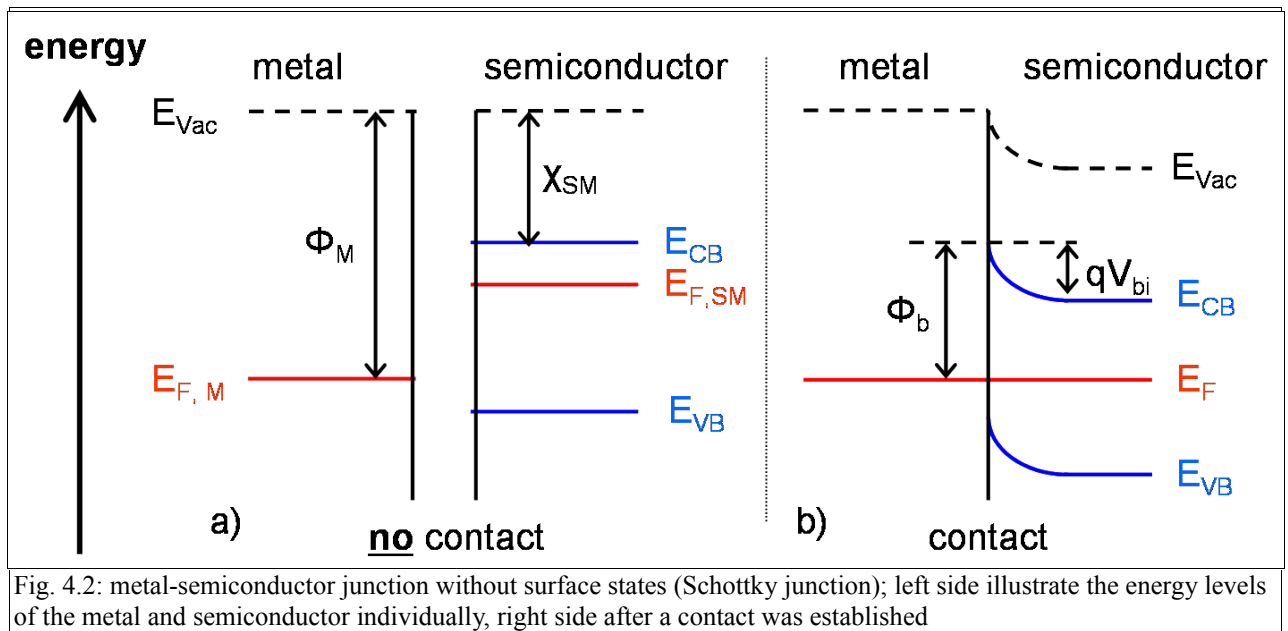
4.2 Semiconductor/metal junction

The semiconductor-electrolyte junction is closely related to the semiconductor-metal junction because both metal and electrolyte have a much higher density of states (DOS) compared to the semiconductor. The space-charge (depletion) region in the metal/electrolyte can be typically neglected. For this reason the semiconductor-metal junction is discussed first and then differences to the semiconductor-electrolyte junction are pointed out.

In general, whenever a semiconductor is in contact with a metal, an energy barrier builds up at the interface. If an ideal metal and semiconductor are considered, this barrier is called Schottky-barrier (also Schottky-diode) after the German physicist Walter H. Schottky [141]. In Fig. 4.2, the example of a n-doped semiconductor and a metal is shown. Typically the Fermi level of a n-doped semiconductor is above the Fermi level of the metal.

The Fermi level of the semiconductor is close to its conduction band and some electrons are thermally excited from electron donors to the conduction band (Fig. 4.2 a). If the semiconductor and the metal are contacted (Fig. 4.2 b), electrons from the conduction band of the semiconductor start to flow to the metal until a common Fermi level has built up. The positively charged donor atoms in the semiconductor remain fixed and a space-charge region develops. Both conduction band and valence band are bent. The number of donors in the semiconductor determines the thickness of the space-charge region.

The positive charge of the donor atoms in the semiconductor is compensated by a negative charge in the metal. Since the density of states in the metal is much higher compared to the semiconductor, the depletion layer is very thin and is restricted to the surface basically. As a consequence the built-in field V_{bi} drops entirely within the semiconductor.



The Schottky-diode is a rectifying contact. Under forward bias the energy barrier qV_{bi} has to be compensated, which is about 400 mV for silicon and 200 mV for germanium. By applying a negative potential to the semiconductor, the depletion layer is shortened and the built-in field qV_{bi} decreases.

Under reverse bias the energy barrier Φ_b has to be compensated. However, if a positive potential is applied to the semiconductor, the depletion region is enlarged and the barrier height increases.

As a first approximation the barrier height Φ_b can be calculated by

$$\Phi_b = \Phi_M - \chi_{SM} \quad (4.1)$$

where Φ_M is the work function of the metal and χ_{SM} the electron affinity of the semiconductor.

Under forward bias mainly four different transport mechanism can contribute to the overall current from the semiconductor to the metal [142]:

- 1) thermionic emission: electrons overcome the energy barrier qV_{bi} by their thermal energy.
- 2) tunneling: especially for a small depletion region and a high doping level of the semiconductor, electrons might tunnel through the energy barrier qV_{bi}
- 3) If the barrier Φ_b is high and the doping level within the semiconductor low, electron/hole

recombination contribute to the forward current

- 4) Holes are injected into the semiconductor and recombine with electrons from the conduction band

According to equation 4.1 the barrier Φ_b should be direct proportional to the work function of the metal. However, in reality, the dependence of Φ_M on Φ_b is mostly weak and especially for covalent semiconductors it is negligible. Bardeen has developed a theory [143] that includes surface trap states in the semiconductor into the analysis to explain the missing correlation.

In the flat band situation (Fig. 4.3 a) the surface trap states are not in equilibrium with the bulk. The Fermi level of the surface electrons $E_{F,sur}$ (occupied surface states are green, unoccupied are black) is lower than the Fermi level in the bulk of the semiconductor $E_{F,bulk}$. If bulk and surface equilibrate, electrons flow from the bulk to the surface. The surface is then charged negatively and next to it, a space-charge region builds up in the bulk (Fig. 4.3 b).

If the semiconductor is then contacted with a metal (Fig. 4.3 b), the electron exchange takes place almost exclusively between the surface states and the metal. The build-in field qV_{bi} and the Fermi level in the semiconductor are only affected a little bit. As a consequence the barrier height Φ_b is mostly determined by the surface properties of the semiconductor and not by the work function of the metal.

In the limit of an infinitely high surface state concentration, the Φ_b does not depend on the work function of the metal at all.

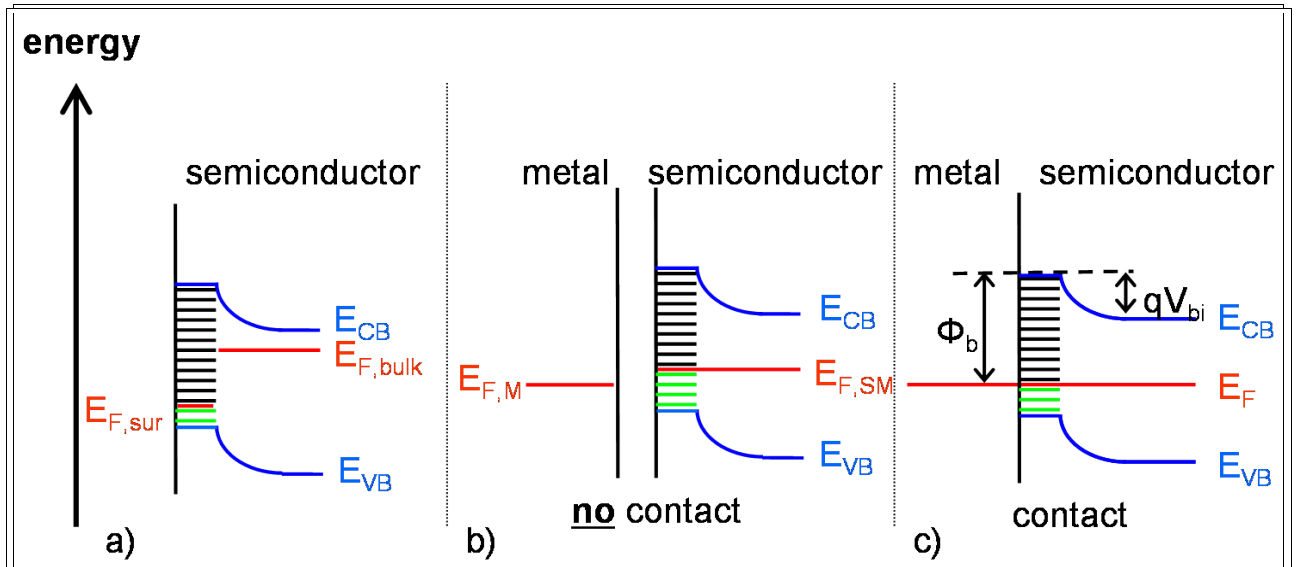


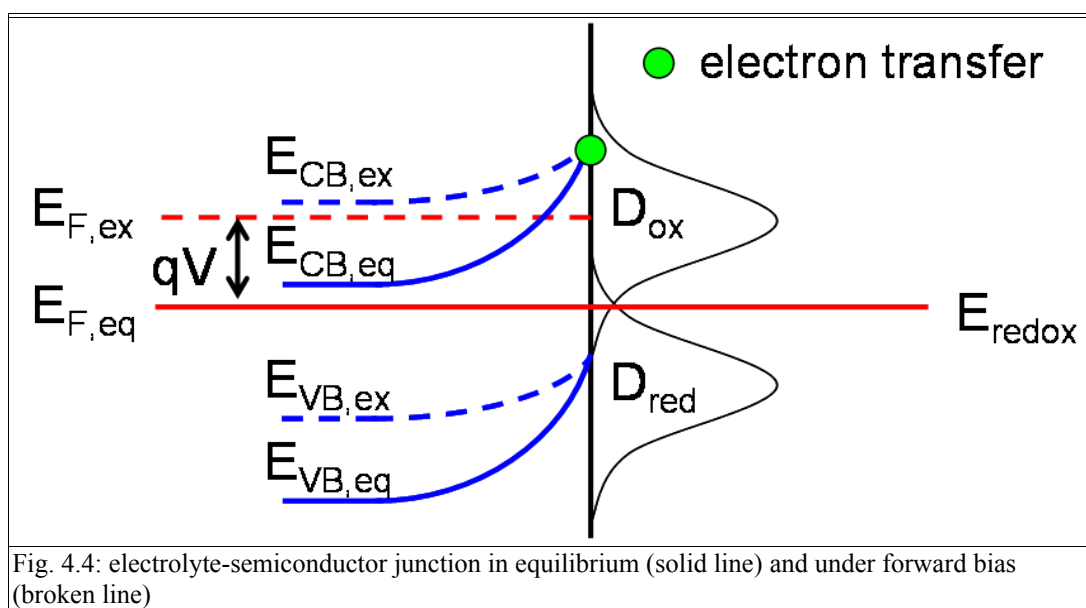
Fig. 4.3: metal-semiconductor junction with surface states (Bardeen junction); from left to right: a) flat band situation (no equilibrium) b) band bending after equilibration c) energy scheme after contact to a metal

The Schottky-barrier and the Bardeen-barrier are theoretic limits, which cannot be used to determine the barrier height Φ_b for real devices. The Schottky-barrier would predict $d\Phi_b/d\Phi_M = 1$, whereas the Bardeen-barrier $d\Phi_b/d\Phi_M = 0$. When using metals with different work functions, many semiconductor-metal junctions exhibit a linear dependence of the barrier height Φ_b on the metal work function Φ_M , but $0 < d\Phi_b/d\Phi_M < 1$. The factor of proportionality is then fitted to determine the barrier height Φ_b .

4.3 Semiconductor/electrolyte junction

The energy scheme of a n-doped semiconductor in an electrolyte with some redox couple Ox/Red looks very similar to a semiconductor-metal junction (Fig. 4.4). Since the density of states in the electrolyte ($D_{\text{ox}}/D_{\text{red}}$) is much higher compared to the semiconductor the depletion layer builds up only in the semiconductor. Electrons diffuse from the semiconductor into the electrolyte until the Fermi level in both semiconductor and electrolyte has equilibrated. The electrical double layer in the electrolyte is only a few Angstrom thick.

In the model from *Helmholtz*, the electrical double layer is treated as a capacitor. Between the positively charged semiconductor and the negatively charged electrolyte a linearly decreasing electric field builds up. The charge carriers in the electrolyte are on fixed positions and have no kinetic energy. This model was extended by *Gouy* and *Chapmann*. They included that ions in the electrolyte can diffuse. Thus the electric field does not decrease linearly but exponentially. However, they treated the ions as being point-shaped so they can approach the electrolyte/semiconductor interface infinitely close. *Stern* merged the ideas of *Helmholtz* and *Gouy/Chapmann* by assuming that the ions cannot approach the interface closer than their radius r_{ion} but may diffuse for a distance $d > r_{\text{ion}}$. As a consequence the electric field decreases linearly for $0 < d < r_{\text{ion}}$ and exponentially for $d > r_{\text{ion}}$. A good introduction on the electrical double layer in the electrolyte/semiconductor interface is given in [144].



In the following the electron transfer from the semiconductor into the electrolyte according to *Gerischer* is briefly discussed [145]. If oxidized redox species in the electrolyte are reduced by conduction band electrons, a potential barrier at the semiconductor/electrolyte interface has to be overcome. Since that barrier is very thin it can be tunneled. Under the assumptions that the electron transfer is non-radiative, the initial and final state must have the same energy.

The transfer rate j_{el} for the anodic current depends on the density of occupied states in the conduction band of the semiconductor N_{CB} and the density of the unoccupied states in the electrolyte D_{Ox} at the energy where the electron transfer takes place, a tunneling probability ρ_{el} and a transition frequency $\nu_{el}(E)$.

$$j_{el} = \int_0^{\infty} \nu_{el}(E) * \rho_{el} * N_{CB}(E) * D_{Ox}(E) dE \quad (4.2)$$

The corresponding expression for the cathodic current is

$$j_h = \int_0^{\infty} \nu_h(E) * \rho_h * N_{VB}(E) * D_{Red}(E) dE \quad (4.3)$$

The electron concentration N_{CB} depends on the density of states DOS_{CB} multiplied with the occupation probability $f(E)$, which is given by the Fermi-Dirac distribution.

$$N_{LB} = \int_{E_c}^{E_{max}} f(E) * DOS_{CB}(E) dE \quad (4.4)$$

The energy distribution of the occupied/unoccupied density of states D_{Ox} , D_{Red} is gaussian shaped, which reflects the impact of the solvent molecules on the energy of the dissolved ion (Fig. 4.5). The interaction between the ion and the solvent is mainly electrostatic. The average distance between the

ion and the dipole of the solvent molecule will determine its energy. Around the equilibrium state the energy as a function of ion-dipole distance is parabolic. The occupation probability is determined by the Boltzmann distribution and decreases exponentially with increasing energy.

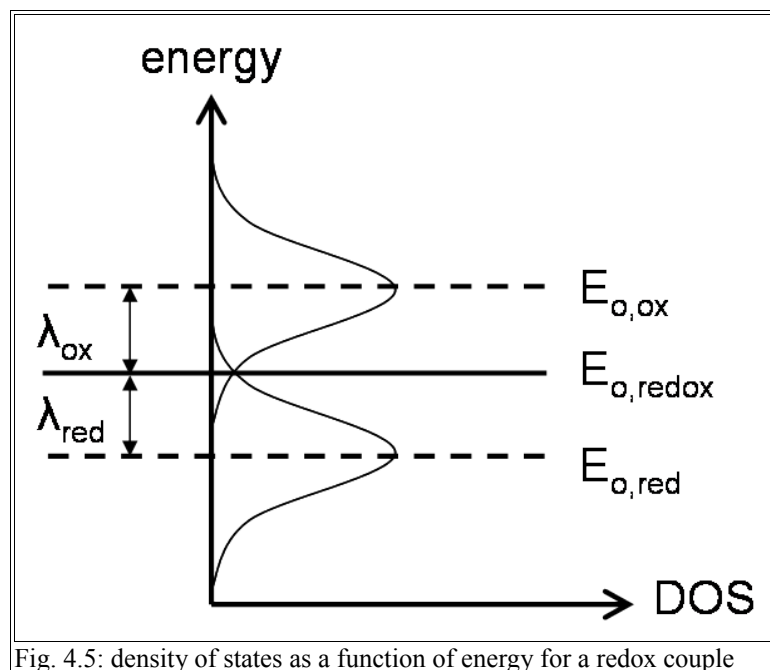


Fig. 4.5: density of states as a function of energy for a redox couple

An electron exchange between the oxidized and reduced redox species follows the Franck-Condon principle. It says that due to the lower mass of an electron the position of the nuclei is assumed to be fixed in the electron transfer process. Since the equilibrium configuration of the solvent molecules is different for the oxidized and reduced ion, the solvent molecules have to reorganize after the electron transfer associated with a reorganization energy λ_{ox} and λ_{red} .

4.4 Electron transport in dye sensitized solar cells

Two dissenting explanations for the working principle of dye sensitized solar cells exist in the literature, which are discussed briefly in the following. The so-called kinetic model [146] neglects the presence of any built-in field in the device whereas the junction model emphasize the importance of a built-in field at the FTO/TiO₂-interface [147].

1) kinetic model

The name of the model expresses that only kinetic parameters determine the incident photon to electron conversion efficiency (IPCE) of the device. The electron injection from the excited dye into the TiO₂ conduction band occurs in the femtosecond range [148] and the reduction of the oxidized dye in about 10⁻⁸ s [131]. The recombination reaction of conduction band electrons with the electrolyte is in the microsecond range (chapter 6.3.3) and thus at least five orders of magnitude slower. Together with the high diffusion coefficient of electrons in the nanoporous TiO₂-network (ca. 1.5*10⁻⁵ cm²s⁻¹ [149]) this is believed to be the origin for the high charge extraction probability.

After electron injection, the electron density in the TiO₂ conduction band increases, shifting the electron's quasi-Fermi level E_F to higher energy while the redox potential of the electrolyte E_{redox} remains almost unchanged due the high concentration of charge carriers. The quasi-Fermi level is the sum of the chemical potential μ_{el} and the electrostatic potential ϕ_{el} times the elementary charge q .

$$E_F = q * \phi_{\text{el}} + \mu_{\text{el}} \quad (4.5)$$

The chemical potential μ_{el} is greatly affected by the injection of additional electrons while the electrostatic potential remains nearly the same [150]. For this reason band edge movement is typically considered to be negligible.

The chemical potential is converted to an electrostatic potential at the TiO₂/FTO front

contact. Thus the maximum attainable open circuit potential is defined as the difference between the quasi Fermi E_F level of electrons in the TiO_2 conduction band and the redox potential of the electrolyte E_{redox} [146].

2) junction model

In contrast to the kinetic model, the junction model is based on an electrostatic approach [147]. Though it agrees with the kinetic model, that no electric field is present in the bulk of the TiO_2 -layer due to the dimensions of the TiO_2 -particles, an in built-electric field at the TiO_2/FTO interface is required in the dark. It originates from the difference of the FTO-work function ϕ_{FTO} and the redox potential of the electrolyte E_{redox} and an insufficient electrostatic screening inside the TiO_2 . Some theoretical modeling has been undertaken to determine the electrostatic potential distribution at the interface for a simplified geometry, in which TiO_2 -cylinders are oriented perpendicular to the FTO-substrate [151][152]. The maximum attainable open circuit potential in this model corresponds to the difference between the FTO work function ϕ_{FTO} and the redox potential E_{redox} .

As a consequence the open circuit potential should depend on the work function of substrate. However, for different substrates (F:SnO₂, Al:ZnO, Al, Au) with a difference of the work function of up to 800 mV, almost no difference in the open circuit potential has been found [153], for which the junction model has been criticized for.